

Behaviour of Bentonite Clay in Toxic Waste Barriers –QuantiSci

1 Introduction

The disposal of toxic and radioactive waste requires a great deal of care and foresight; it is inherently a long timescale problem. The application presented by *QuantiSci Ltd.* at the European Study Group with Industry 1998, concerns toxic waste being buried underground, surrounded by layers of bentonite, a form of very pure clay with 10–20nm platelets. This type of clay is chosen because of its extremely low permeability owing to its platelet size and high water absorption qualities. The environment of the burial site is usually at several hundred metres below the water table in a drilled tunnel surrounded by rocks with small fracture features.

The bentonite is placed, typically with 50% saturation, into the drilled tunnel around a canister containing the waste material (Fig.1). Owing to the initially partial saturation

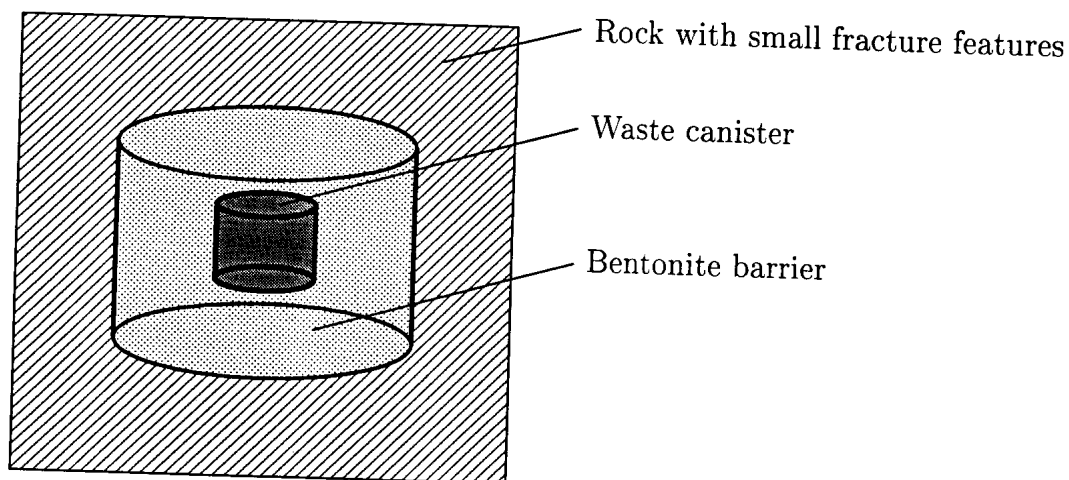


Figure 1: Layout of bentonite barrier within rock

of the bentonite, very large capillary and electrochemical forces are developed during the

saturation process — compressing the platelets and thereby inducing large swelling pressures approximately an order of magnitude greater than the hydrostatic pressure. These high swelling pressures cause the bentonite to migrate into the fractures of the surrounding rock, reducing the swelling but also removing material from the protective shield of the clay around the waste canister. The extruding bentonite changes behaviour in the fractures, with the outer tips becoming less viscous and becoming more like a gel.

QuantiSci explicitly posed two questions to the Study Group participants:

1. What can be said about the motion of the clay into the cracks? How far does it travel? Does it reach a steady state, and if so, when?
2. At which rate do clay particles at the tip of the clay intrusion dissolve into the adjacent water, allowing for a leaching away of the clay?

The purpose of this report is to investigate these questions. Although it is not easy to give a complete answer to the second question, we can easily estimate an upper bound on the loss of material, and we present this estimate first. After that, in sections 3-7 we discuss the first question.

2 Leaching of clay particles

At the tip of the clay intrusion, the dilute mixture of clay and water creates a gel-like substance. One can imagine clay particles dislodging themselves from this gel and being transported through the water ahead of the clay via convection and diffusion. On long time scales such a loss of particles might pose a threat to the integrity of the clay barrier.

The rate of this leaching process can be limited by either of two subprocesses: the dissolution of the particles at the gel-water interface and the subsequent transport process. Having not been able to find experimental data on the rate of dissolution, we assumed— in order to obtain an upper bound on the total rate—that the dissolution is more rapid than the transport, and that therefore the transport process limits the rate of the whole process. The rate of diffusivity of the clay particles in water, given by the Stokes-Einstein relationship ($D = 5 \cdot 10^{-5} \text{ m}^2/\text{yr}$) then allows us to calculate the total mass flux as a result of this transport.

We denote by $c [\text{t}/\text{m}^3]$ the concentration of the particles in the water, and let $x [\text{m}]$ parametrize the crack, with $x = 0$ corresponding to the tip of the intrusion. For the choice of domain there are two alternatives: either we assume the crack to be infinite, which corresponds to $c = 0$ at $x = x_0 = \infty$, or we suppose that the crack intersects with a larger crack at, say, $x = x_0 < \infty$.

Since we assumed the dissolution process to be rapid in comparison to the transport process, we expect to see at $x = 0$ values of c close to the saturation concentration c_0 . The

concentration c is then governed by the equation

$$\begin{aligned}\frac{\partial c}{\partial t} - D \frac{\partial^2 c}{\partial x^2} &= 0 & 0 < x < x_0, t > 0 \\ c(0, t) &= c_0 & t > 0 \\ c(x, 0) &= 0 & 0 < x < x_0.\end{aligned}$$

If $x_0 = \infty$, the concentration c is given by

$$c(x, t) = c_0 \operatorname{erfc} \left(\frac{x}{2\sqrt{Dt}} \right) \quad (1)$$

and the total loss of mass is given by the total flux through the boundary $x = 0$ between $t = 0$ and $t = T$,

$$\frac{c_0 \sqrt{D}}{\sqrt{\pi}} \int_0^T \frac{dt}{\sqrt{t}} = \frac{2c_0 \sqrt{D}}{\sqrt{\pi}} \sqrt{T}.$$

For the case of a bounded crack, the concentration profiles are given by (1) for small times, but for large times converge to the stationary state

$$c_\infty(x) = c_0(1 - x/x_0).$$

This stationary state has a mass flux at the origin of Dc_0/x_0 .

As an example we assume that the canisters are deposited in a cylindrical hole with diameter 4 m and height 3 m, so that the total volume is $V = 37.7 \text{ m}^3$ and the lateral surface area is $A = 37.7 \text{ m}^2$. If we suppose that of that surface area 10% consists of crack aperture, and that the concentration at the tip of the extrusion is equal to $c_0 = 0.01 \text{ t/m}^3$, then the mass losses after time T in the two cases are estimated (from above) by

$$\begin{aligned}\frac{2c_0 \sqrt{D}}{\sqrt{\pi}} 0.1A \sqrt{T} &= 1.7 \cdot 10^{-4} \text{ t } \sqrt{T/\text{yr}} && \text{for the infinite crack} \\ \frac{c_0 D}{x_0} T &= 5 \cdot 10^{-8} \text{ t } T/\text{yr} && \text{for a crack of length 10 m.}\end{aligned}$$

3 Swelling Pressure

The basic driving force in the extrusion process is the property of clay to adsorb water and consequently swell, possibly against high pressure gradients. A measure of this property is the *swelling pressure*, P_{sw} , which is defined as the difference between bulk clay pressure and pore water pressure in water-saturated (no air or voids) clay.

Pusch (1991) supplied numerical data on this swelling pressure (Figure 2) as well as the curve that was fitted to this data,

$$P_{\text{sw}}(\rho) = 3.06 \cdot 10^{-9} \text{ MPa } \exp(10.938 \rho/\rho_w), \quad \rho_w = 1 \text{ t/m}^3. \quad (2)$$

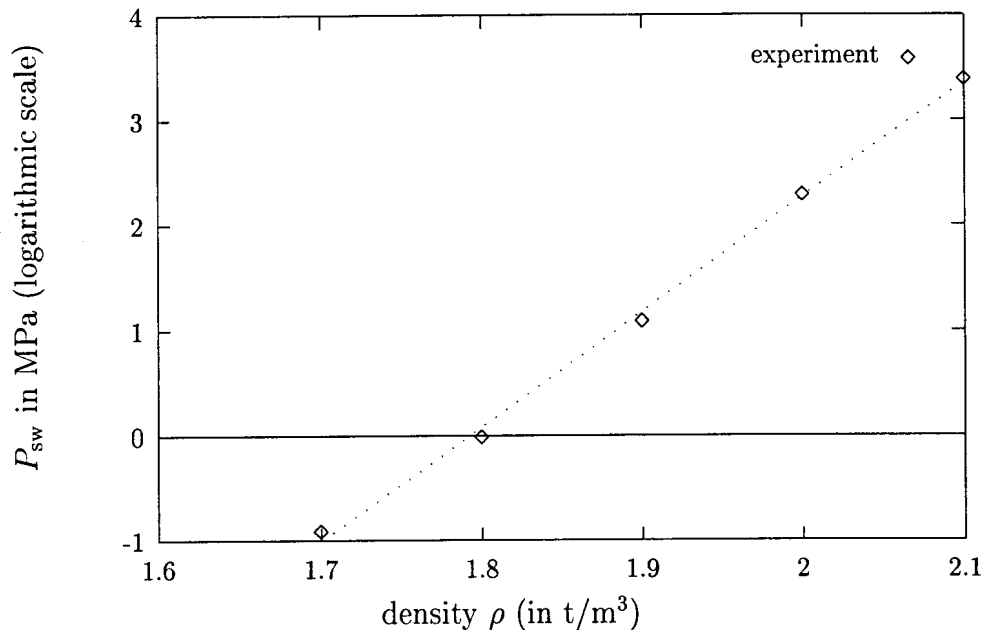


Figure 2: Swelling pressure *vs.* density Pusch (1991)

(Note that since the clay is supposed to be saturated with water, there is a one-to-one correspondence between values of ρ and the mixing ratio of clay particles and water). It is important to observe that this numerical data does not include the dilute range, where the density ρ is close to that of water (1 t/m^3). From the discussion that follows, the behaviour of the extruded clay is strongly dependent on the values of P_{sw} in this range.

4 Model I: Mass Balance

In a practical situation the movement of clay and water consists of two phases, which may overlap each other. Initially the clay is only partially saturated with water, and any water that enters the burial space will be adsorbed by the clay, driving out the air. In this process the clay expands to fill the whole space surrounding the canister.

In the second phase the clay is still adsorbing water, but its volume is confined and therefore the bulk pressure of the clay increases. This increased pressure will result in the clay extruding into cracks and fractures in the rock wall.

These two phases may in principle overlap each other, since the clay swells most at the outer boundary, where it is in contact with the incoming water. If the water does not spread fast enough through the clay, the pressure might increase locally and cause extrusion while other parts of the clay have not yet reached saturation.

If the movement of the pore water in the clay is governed by Darcy's Law, subject to pressure gradients given by the swelling pressure, then the dispersal of water is indeed a slow process (see Section 7). However, observations show that the equilibration of water

happens much faster than this, and in fact takes place on a time scale that is short with respect to the extrusion. Based on these experiences, we leave the problem of the initial swelling aside and assume that the clay has swollen to maximum.

Under some simplifying hypotheses we can make a rough estimate of the extrusion process based on mass balance.

The observation that water equilibrates quickly throughout the clay suggests that in the core (the region between the canisters and the rock wall) the density of the clay is homogeneous throughout the evolution. Consequently the pressure in the core, which is equal to the pressure of the surrounding pore water, P_0 , plus the swelling pressure $P_{sw}(\rho)$, is also constant. This pressure creates a movement of the clay into the cracks.

The movement of the clay itself causes an expansion of the volume occupied by the clay, and therefore a decrease in bulk pressure. As a consequence water enters via the cracks—the same cracks through which extrusion takes place—and causes the core clay to regain equilibrium, at a lower density (and therefore at a lower swelling pressure).

To estimate the rate at which this process takes place, we suppose that there is a homogeneous distribution of cracks (at least of those that are important for this process—probably only those of diameter $d > 0.1$ mm Pusch (1991) and in each crack a definite front at location $x = s(t)$ (see Figure 3). At any time $t > 0$ the total volume of the clay is

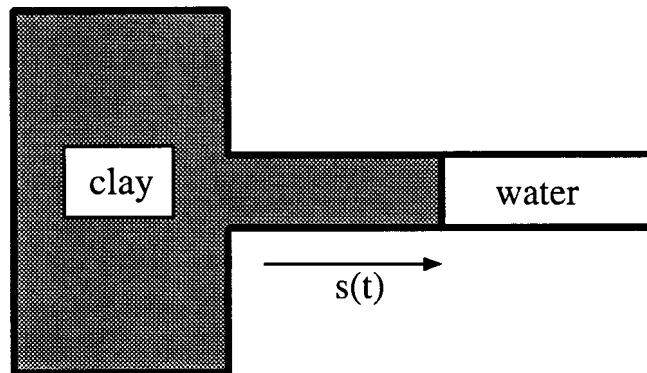


Figure 3: The crack geometry.

given by the initial volume V_0 plus the volume occupied in the cracks:

$$V(t) = V_0 + v(s(t)) \quad (3)$$

and for the mass at time t we have

$$M(t) = M_0 + v(s(t))\rho_w, \quad (4)$$

where $\rho_w = 1 \text{ t/m}^3$ is the density of water. The function $v(s)$ (units m^3) takes account of the different possible crack geometries. If we think of a ‘one-dimensional’ crack, then

$v(s) = As$, where A is the total aperture; however, if the repository is cylindrical with radius r , then v takes the form

$$v(s) = \frac{A}{2\pi r} \pi((r+s)^2 - r^2).$$

Whatever the geometry, the density of the clay in the core is then given by

$$\rho(t) = \frac{M(t)}{V(t)}. \quad (5)$$

The difference between the pressure of the water in the cracks, P_0 , and the pressure of the core clay, $P_0 + P_{sw}$, drives the clay into the cracks. Assuming a constant viscosity¹ μ , the movement of the interface is given by a Poiseuille-type flow law,

$$\dot{s}(t) = \frac{d^2}{12\mu} \frac{P_{sw}(\rho)}{s(t)}. \quad (6)$$

Since ρ is a function of $s(t)$ by equations (3), (4), and (5), this equation completely defines the location of the interface $s(t)$.

5 Stationary states and long-term behaviour

Assuming a long-term view, an important question is the final extent of the extrusion. Equation (6) is of the form

$$\dot{x} = f(x), \quad x(0) = 0, \quad f(0) > 0,$$

and the solution $x(t)$ of this problem increases up to the first value x_0 where $f(x_0) = 0$. If no such value exists, then $x(t)$ is unbounded. In equation (6) the right-hand side can only vanish if P_{sw} vanishes at a certain value of ρ —implying that at that density the clay has the same equilibrium pressure as the surrounding water. The data presented in Figure 2 do not contain enough information to decide whether this is the case or not; certainly the formula (2) that is fitted through the data points suggests that $P_{sw}(\rho) > 0$ for all $\rho > 1$. We suggest that accurate measurements of the swelling pressure near $\rho = 1$ be made (or found).

It is important to note here that the limit situation is determined by a simple stopping criterion,

$$P_{sw}(\rho) = 0.$$

This criterion is independent of assumptions on the variation of the viscosity with ρ , or on the exact type of the flow inside the crack. It is even independent of the thickness of the crack.

¹This is incorrect for at least two reasons: first, at constant temperature the viscosity depends strongly on the density of the clay; secondly, clay is a nonlinear viscous material. However, for the question of the ultimate length of the extrusion, the viscosity plays no role (except for the possible yield shear stress).

The properties of clay suggest an alternative mechanism that might limit the extent of the extrusion. Bentonite is widely reported to have a yield shear stress τ_c , below which the material acts as a solid. Such a material can only move through a crack of width d if the pressure drop Δp over a length L satisfies

$$\frac{d}{2} \frac{\Delta p}{L} > \tau_c.$$

This presents a new stopping criterion: extrusion will continue until

$$\frac{P_{sw}(\rho)}{s} = \frac{2}{d} \tau_c. \quad (7)$$

From this criterion we can distill two limit cases. If there are few cracks, so that the volume increase and therefore the change in ρ and P_{sw} are small, then (7) indicates that the extrusion will stop because the pressure drop is distributed over a large length of crack. At the other end of the scale, if there are many cracks, then the volume and density vary strongly in the extrusion process, and the decrease in P_{sw} might be the main effect in satisfying (7).

In order to test this hypothesis we compare the experimental results of Kanno & Wakamatsu (1983) with the prediction of (7). Using the cylindrical geometry of the experiment and taking a yield shear stress² $\tau_c = 500$ Pa, we find a final extrusion length of 11 mm for a crack of width 1.5 mm, whereas the experimental result was approximately 20 mm.

6 Model II: Lubrication approximation

The modelling of the movement of clay in the crack as presented above is very simple. A more faithful representation can be found by considering the flow in the crack as a two-dimensional flow (for a planar crack) or in the case of a cylindrical pore an axially symmetric flow, and subsequently simplifying the equations by applying a lubrication approximation. In this section we concentrate on the flat crack case.

Assuming the clay to be a viscous compressible Newtonian fluid, the governing equations in the crack are

$$\frac{\partial \rho'}{\partial t'} + \nabla \cdot (\rho' \mathbf{u}') = 0 \quad (8)$$

$$\frac{d\mathbf{u}'}{dt'} = -\nabla P'_{sw} + \mu'(\rho') \nabla^2 \mathbf{u}' + (\lambda + \mu) \nabla(\nabla \cdot \mathbf{u}') \quad (9)$$

$$P'_{sw} = f(\rho'), \quad (10)$$

where primes denote dimensional quantities.

²This number is not based on measurements on bentonite, but a wild guess based on comparison with completely different materials. In addition, the yield stress has been shown to be small (~ 1 Pa) at low densities, Pusch (1991). A good experimental measurement of the yield stress would be very valuable.

If the clay occupies a narrow crack, $z \in [-H, H]$, with a typical length-scale L , then the standard lubrication scaling for this system is

$$x' \rightarrow Lx, \quad z' \rightarrow Hz = \delta Lz, \quad \rho' \rightarrow \rho_0 \rho, \quad u' \rightarrow Uu, \quad t' \rightarrow (L/U)t, \quad \mu'(\rho') \rightarrow \mu_0 \mu(\rho)$$

where ρ_0 , U , and μ_0 are the density, velocity, and viscosity scales. The continuity equation (8) then requires $w \rightarrow \delta U w$. This leaves the continuity equation unchanged. To prevent a non-trivial solution, the x component of (9) requires a pressure scaling $P'_{sw} \rightarrow (\mu_0 U / \delta^2 L) p$ (since $\delta \ll 1$ this scaling indicates the lubrication pressures are very high). The Navier-Stokes equations become

$$0 = -\frac{\partial p}{\partial x} + \frac{\partial}{\partial z} \left(\mu(\rho) \frac{\partial u}{\partial z} \right) + O(\delta^2, \delta^2 Re) \quad (11)$$

$$0 = -\frac{\partial p}{\partial z} + O(\delta^2, \delta^2 Re), \quad (12)$$

whilst (10) becomes

$$p = \frac{\delta^2 L}{\mu_0 U} f(\rho_0 \rho) = F(\rho). \quad (13)$$

Provided $O(\delta^2)$, $O(\delta^2 Re) \ll 1$ these terms are negligible and (11), (12) are, to leading order, the standard equations for lubrication theory. Equation (12) indicates that the pressure, to leading order, is independent of z , as is ρ , by virtue of (13). Equation (11) then integrates immediately, subject to no-slip conditions on the walls ($u(\pm 1) = 0$),

$$u = \frac{1}{2\mu(\rho)} \frac{\partial p}{\partial x} (z^2 - 1). \quad (14)$$

Substituting this into (8), with $w(\pm 1) = 0$, and integrating over the crack leads to

$$2 \frac{\partial \rho}{\partial t} + \frac{\partial}{\partial x} \left(\rho \int_{-1}^1 u dz \right) = 2 \frac{\partial \rho}{\partial t} - \frac{\partial}{\partial x} \left(\frac{2\rho}{3\mu(\rho)} \frac{\partial p}{\partial x} \right) = 0. \quad (15)$$

The pressure-density relation (10) means that (15) can be expressed equally well in terms of pressure or density. However, removing pressure from the equation leads to the most familiar form

$$\frac{\partial \rho}{\partial t} - \frac{\partial}{\partial x} \left(\frac{\rho}{3\mu(\rho)} \frac{\partial F}{\partial \rho} \frac{\partial \rho}{\partial x} \right) = 0, \quad (16)$$

which is a diffusion equation with a density-dependent diffusion coefficient.

To solve (16) two boundary conditions are required. These and the initial condition are

$$p(0, t) = p_0(t), \quad p(s(t), t) = 0, \quad p(x, 0) = 0, \quad (17)$$

which state that the pressure is known (and varying with time) at the crack entrance, the pressure falls to zero (ambient) at the clay tip, and initially the pressure in the crack is zero. Equation (13) can be used to convert these to density conditions.

In the same way as in the previous model we wish to take into account that the loss of clay into the crack reduces the density of the remaining clay in the core. Therefore the swelling pressure in the core, the driving force behind the extrusion, also reduces. At time $t > 0$ the total mass in the crack has increased by (in dimensional quantities)

$$\int_0^\infty (\rho'(x', t') - \rho_w) \frac{\partial v'}{\partial x'}(x') dx',$$

where $v'(x')$ is the same function (apart from the extra prime to denote dimensionality) as in equations (3) and (4). Since the total mass in the system is constant, this implies that the mass of the core has decreased by the same amount. Consequently the density in the core at time T equals

$$\rho'_c(t') = \frac{1}{V_0} \left(M_0 - \int_0^\infty (\rho'(x', t') - \rho_w) \frac{\partial v'}{\partial x'}(x') dx' \right). \quad (18)$$

At the crack entrance the pressure is then given by this density and (13):

$$p(0, t) = F(\rho_c(t)) \quad \text{or equivalently} \quad \rho(0, t) = \rho_c(t). \quad (19)$$

Numerical calculations have been performed to determine the profiles of solutions $\rho(x, t)$ of this equation. We assume linear crack geometry, so that $v'(x') = Ax'$, where A is the total aperture of the cracks. Equation (18) can be written in the more convenient (dimensionless) form

$$\frac{\partial \rho_c}{\partial t} = -\frac{LA}{V_0} \int_0^\infty \frac{\partial \rho}{\partial t} dx,$$

We assume here that we can choose $LA/V_0 = 1$ without violating the smallness constraints on $\delta = H/L$ (see above). This yields on substitution of equation (16),

$$\frac{\partial \rho_c}{\partial t} = -\frac{\rho}{3\mu(\rho)} \frac{\partial F}{\partial \rho} \frac{\partial \rho}{\partial x} \Big|_{x=0}. \quad (20)$$

Writing

$$\kappa(\rho) = \frac{\rho}{3\mu(\rho)} \frac{\partial F}{\partial \rho}(\rho), \quad (21)$$

we solve the equation

$$\frac{\partial \rho}{\partial t} - \frac{\partial}{\partial x} \left(\kappa(\rho) \frac{\partial \rho}{\partial x} \right)$$

with boundary conditions given by (19) and (20). As initial value for ρ_c was taken 1.8.

For the function κ two different forms were taken. Pusch (1991) [p. 37] mentions the viscosity function

$$\mu(\rho) = e^{20(\rho-1)}.$$

If $p(\rho) = e^{9\rho}$, as suggested by the data mentioned above, then an appropriate choice of κ would be

$$\kappa(\rho) = 9\rho e^{-11\rho} \quad (\text{Case 1}).$$

Figure 4 shows ρ as a function of x for this function κ . The plotted curves correspond to

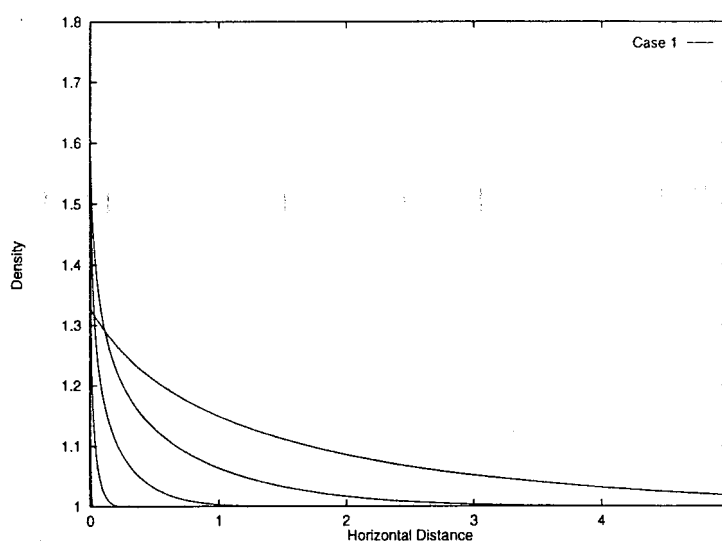


Figure 4: ρ vs. x for $\kappa(\rho) = 9\rho e^{-11\rho}$.

(dimensionless) times $t = 5000, 10000, 15000,$ and 20000 . Using the relation $L = V_0/A$ and the typical flow rate U (given by the choice of κ , combined with (21) and (13)) these numbers can be made dimensional. Note that κ is largest near the tip of the intrusion, and that therefore the largest resistance to the flow is at the entrance of the crack.

The measurements of p and μ do not cover the values of ρ near ρ_w . To judge the influence of the uncertainty in this region, we also performed the calculations for the function

$$\kappa(\rho) = 9\rho e^{-11\rho} \tanh(10(\rho - 1)) \quad (\text{Case 2}). \quad (22)$$

The difference between the two functions is less than 0.1% if $\rho > 1.4$. The result is shown in Figure 5. Figures 6 and 7 show the density of the clay in the core (ρ_c) and the position of the tip of the intrusion in the two cases. Note that since in the case (22) $\kappa(1) = 0$, there is a well-defined front; in the case of $\kappa(\rho) = 9\rho e^{-11\rho}$, the front is defined as the location of the density level 1.0001.

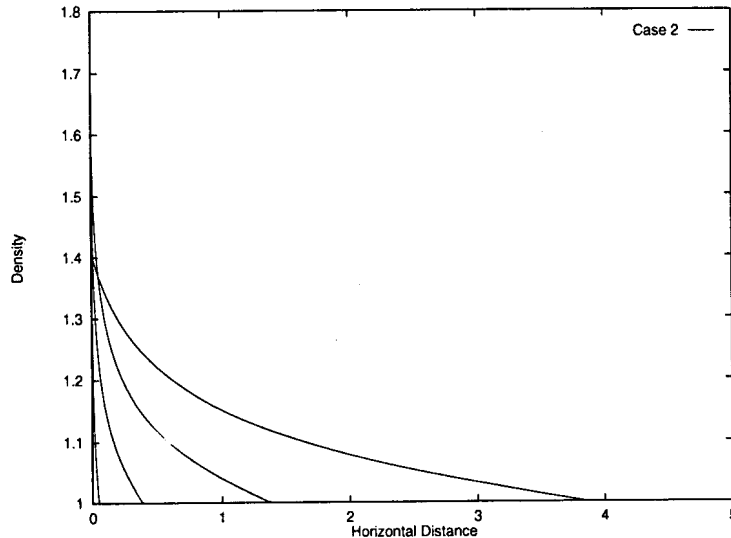


Figure 5: ρ vs. x for $\kappa(\rho) = 9\rho e^{-11\rho} \tanh(10(\rho - 1))$.

Equation (16) describes the flow of a Newtonian fluid. However, bentonite is well known to behave as a Bingham fluid, so (16) can at best be used to estimate solutions above the yield stress. A more realistic model, which still is easily implemented, is to describe the fluid as shear thinning

$$\tau = \mu \left(\frac{\partial u}{\partial z} \right)^\alpha \quad (23)$$

where τ is the shear stress and $\alpha\mu(\partial u/\partial z)^{\alpha-1}$ is the effective viscosity, $\alpha < 1$. Following through the previous argument, with the Navier-Stokes equations appropriately modified, leads to an equivalent version of (16):

$$\frac{\partial \rho}{\partial t} - \frac{\partial}{\partial x} \left(\frac{\alpha}{1 + 2\alpha} \rho \left(\frac{1}{\mu(\rho)} \frac{\partial F}{\partial \rho} \frac{\partial \rho}{\partial x} \right)^{1/\alpha} \right) = 0. \quad (24)$$

The pressure scaling in this model is $P'_{sw} \rightarrow \mu_0 U^\alpha L / H^{\alpha+1} p$. Note that the limit $\alpha \rightarrow 1$ reduces (24) to (16).

7 Rapid water movement?

Experimental evidence suggests that the duration of the saturation phase of the clay—when water is sucked in from the surrounding rock, and air is driven out—is of the order of tens of years. This contrasts with a simple calculation based on Darcy's law, using a typical value of the permeability of clay, $k = 10^{-20} \text{ m}^2$. Supposing a clay layer of 1 m

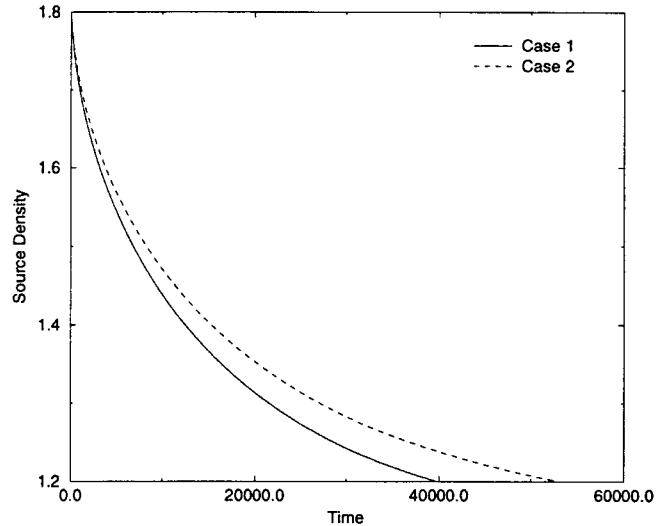


Figure 6: Density of the clay remaining in the core ($\rho_c(t)$).

thickness and a pressure drop over the width of 20 MPa, we find a velocity of

$$u = -\frac{k}{\mu} \nabla p \approx 10^{-2} \frac{\text{m}}{\text{yr}}.$$

This seems to be too slow for the observational evidence.

There are several possible explanations for this. There may simply be an error in the determination of the permeability, or there may be cracks between the blocks of clay, allowing the water to travel more rapidly between different parts of the repository. At a smaller scale, electrochemical pressures active between the water molecules and the platelets probably orders of magnitude higher than pressures measured on the bulk scale, and these might also give rise to higher flow rates.

8 Summary

In conclusion, we have been able to come up with the following answers to the questions posed:

1. How far does the clay extrude into the rock, and does it reach a steady state?

Answer: We have derived both a simple ODE model (sections 4 and 5) and a more sophisticated PDE model (section 6) that can be used to predict the extrusion profiles and time scales. Neither of the models have steady states, but instead a front velocity that vanishes asymptotically.

2. Estimate the rate of dissolution of clay particles into pore water.

Answer: For the example calculations of section 2, the bentonite mass loss is small relative to the total mass, over time scales up to 10^6 years.

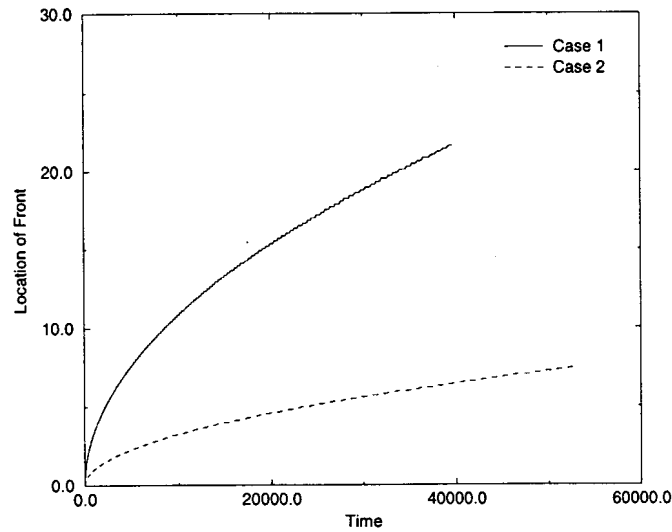


Figure 7: Position of the tip of the intrusion.

References

- Kanno, T. & Wakamatsu, H. (1991) *Experimental study on bentonite gel migration from a deposition hole*, Proc. 3rd Int. Conf. Nuclear Fuel Reprocessing and Waste Management (RECOD '91), Sendai. Pusch, R (1983) *Stability of Bentonite Gels in Crystalline Rock—Physical Aspects*. KBS Technical Report 83-04.

Report submitted by P. Bolchover, T. G. Myers, M. A. Peletier & M. Ahmer Wadee.

Contributions from Gail Duursma, Alistair Fitt, Poul Hjorth, Andrew Hogg, John Lister, David Parker, Colin Please, and Alan Rempel